Available online at www.sciencedirect.com
ScienceDirect
Ceramics International 38 (2012) 235–242
CERAMICS INTERNATIONAL
www.elsevier.com/locate/ceramint

Synthesis, growth mechanism and photoluminescence of monodispersed cubic shape Ce doped YAG nanophosphor

Prabhakar Rai, Min-Kyoung Song, Hyeon-Min Song, Jeong-Hyun Kim, Yun-Su Kim, In-Hwan Lee, Yeon-Tae Yu *

Division of Advanced Materials Engineering and Research Centre for Advanced Materials Development, College of Engineering, Chonbuk National University, Jeonju 561-756, South Korea

Received 1 April 2011; received in revised form 20 June 2011; accepted 28 June 2011
Available online 12th July 2011

Abstract

In the present work, a novel method for the synthesis of monodispersed cubic shape Ce-doped yttrium aluminum garnet (YAG:Ce) nanophosphors is reported. Single phase Ce doped YAG nanoparticles are prepared by solvothermal processing, followed by annealing treatment. Morphological investigation by scanning electron microscopy (SEM) showed the formation of monodispersed 500 nm cubic shape Ce-doped YAG phosphor. The crystalline Ce-doped YAG showed broad emission peaks in the range of 480–640 nm with maximum intensity at 524 nm. The emission intensity increased with increase in calcination temperatures while reduced with increase in Ce^{3+} ions concentration. Detailed study was carried out to understand the formation of monodispersed cubic shape Ce doped YAG nanoparticles. It was found that the solvent, surfactant and impurity (counter ions of cerium and aluminum salt) has significant effect on the crystal growth.

Keywords: A. Powders: chemical preparation; A. Calcination; C. Optical properties; YAG:Ce

1. Introduction

Recent research is focused on the nanocrystalline materials for their considerable potential in technological applications and fundamental properties. As compared to bulk material these nanocrystalline materials exhibit so many novel properties [1]. Recently, inorganic phosphors have been extensively investigated for application in various types of display technologies [2]. Among them Ce-doped yttrium aluminum garnet (YAG:Ce) is an advanced optical material having numerous applications possibilities such as a luminescent material in vacuum ultraviolet (VUV), plasma display panels (PDPs), solid-state lasers, and solid-state lighting, for its high luminescence efficiency and chemical stability [3,4]. YAG:Ce phosphors have been found to be suitable for converting the blue light emitting diode (LED) radiation into a very broad band yellow emission, which can be used as one of the most common methods for producing white light with a gallium nitride-based blue LED [5]. The size reduction of phosphors is found to be the most effective way to improve the LED efficiency because smaller particles possess a higher surface to volume ratio, which enhances the efficiency of absorption and emission. Huang et al. investigated the effect of particle size distribution of YAG:Ce phosphors on packaging performance in white LED applications [6]. The YAG:Ce phosphors with different particle sizes were packaged in white LEDs using different amounts of each phosphor. It was found that for smaller particle sizes a minimal amount of phosphor material was required for efficiency similar to that exhibited by commercially available YAG:Ce phosphors. To improve the brightness and resolution of these displays, much effort has been made to develop phosphors with controlled morphology, high efficiency and fine size particles.

YAG phosphors doped with activators are mainly synthesized by the solid-state reaction techniques [7]. To achieve desired phase purity and required particle size, process of the solid-state reaction usually needs extensive ball milling and lengthy high temperature treatment (~1600 °C) with flux, such as B_2O_3, PbO, and BaF_2, which generally introduces additional impurities and defects [8]. YAG particles have been also

* Corresponding author. Tel.: +82 63 270 2288; fax: +82 63 270 2305.
E-mail address: yeontae@chonbuk.ac.kr (Y.-T. Yu).

0272-8842/$36.00
doi:10.1016/j.ceramint.2011.06.057

produced using several chemical techniques [9–16]. These chemical processes achieve symmetrical mixing of the precursor materials on the molecular level, lowering the synthesis temperature and promoting the formation of submicron and/or nanosized particles having uniform grain morphology. Purwanto et al. reported flame-assisted spray pyrolysis synthesis of agglomerate-free YAG:Ce submicrometer particles and crystals annealed at 1100 °C for a time shorter than 8 h were agglomerate-free spheres [14]. Higher annealing temperature and longer annealing time led to a necking phenomenon and even agglomeration among particles with rougher surfaces. Yang et al. synthesized monodispersed YAG:Ce phosphors by the hydrothermal-homogeneous precipitation method at 100 °C for 4 h and 240 °C for 20 h followed by post annealing at 1200 °C for 2 h [11]. Although they got monodispersed particles in nanometer range but it requires a relatively long duration calcination step involving temperatures in excess of 1100 °C. In this work, we propose a two step method for the synthesis of monodispersed cubic shape Ce doped YAG nanoparticles at relatively low temperature. This is the first attempt about the shape selective synthesis of Ce doped YAG and no other researcher reported the synthesis of monodispersed cubic shape YAG nanoparticles to our knowledge. To achieve our goal, we used the combined effect of co-precipitation and solvothermal method. To understand the formation of monodispersed cubic shape Ce doped YAG nanoparticles, a detailed study was carried out, by changing the several parameters such as water–ethanol ratio, concentration of CTAB and different kinds of surfactants. The importance of two step synthesis process over simple co-precipitation and solvothermal method is also discussed. Further, their photoluminescence property is also studied.

2. Experimental

2.1. Materials

Aluminum nitrate $Al(NO_3)_3{\cdot}9H_2O$ (A.R., Aldrich, 99.9% purity), cerium nitrate $Ce(NO_3)_3{\cdot}6H_2O$ (Aldrich, 99.9%), and yttrium oxide (99.99% High purity chemicals), were used as raw materials. The yttrium nitrate solution was prepared by dissolving Y_2O_3 (7.5-x mmol) in diluted nitric acid (HNO_3), followed by evaporation of the excess acid. After that it was cooled to room temperature, deionized water was added to make up the volume to 50 ml. The aluminum nitrate and cerium nitrate solution was prepared by dissolving $Al(NO_3)_3{\cdot}9H_2O$ (12.5 mmol) and $Ce(NO_3)_3{\cdot}6H_2O$ (x mmol, $x = 0.2$ mmol) in 50 ml deionized water.

2.2. Powder synthesis

The synthesis of Ce doped YAG was carried out by a two step synthesis process. The reason of adopting a two step synthesis process are as follows: (a) though the co-precipitation method is a simple one for the synthesis of Ce doped YAG, it is difficult to control the shape and size of particles [17], while in hydrothermal method we can control the shape and size of the particles but it needs very high temperature and pressure to produce single phase YAG [18]. In order to overcome these two problems, we modified the simple co-precipitation method by using solvothermal treatment of precursor precipitate to obtain the desired morphology. (b) The crystal morphology depends sensitively on several reaction parameters, including temperature, pH, time of growth, impurities (like metal source and its counterion), and the presence (or not) of any complexing agent. In order to avoid the interference of the impurity with the crystal growth, two steps synthesis process was used. In first step, precursor precipitate, using simple co-precipitation method was prepared and in second step solvothermal reaction of precursor precipitate was carried out in the presence of surfactant. Thus, it may reduce the possibility of interference of other kind of impurity with growing YAG crystal and crystal growth depends only on the nature of surfactant and solvent.

In a typical procedure, the respective nitrate solutions were mixed in a container. The solution was precipitated by adding ammonium hydroxide and the solution pH was maintained in the range 8.5–9. The precipitated slurry was aged for 24 h to make the reaction sufficient, and then the suspension was filtered and washed repeatedly with deionized water to remove residual ammonia and nitric ions. Precursor precipitate was then dispersed in 35 ml solvent (20 ml water, 15 ml ethanol) containing 1 mol% of cetyltrimethylammonium bromide (CTAB). Before transferring the solution into autoclave, it was sonicated for few minutes. The solution was transferred into 50 ml autoclave and heated at 180 °C for 12 h. On completion of the reaction, the autoclave was cooled to room temperature. The product was centrifuged and washed several times by water and ethanol and dried at 80 °C for 12 h. The dried powder was heated at 500 °C in a muffle furnace for 5 h. On cooling to room temperature, the solid sample was grounded into fine powder with an agate mortar. The powder was further calcined at different temperatures, i.e. 700, 800, 900, 1000 °C for 2 h in air to obtain the single phase YAG.

2.3. Characterization

The crystal structure of the powder sample was studied by powder X-ray diffractrometer (XRD, D/Max 2005, Rigaku). The composition of the powder was investigated by the Fourier transformation infrared spectroscope (FT-IR, Perkin-Elmer, Spectrum GX). Particle size and morphology was investigated by scanning electron microscopy (SEM-JSM-5900, JEOL). Photoluminescence property (PL) was studied by using a Cd–He laser source with 325 nm excitation.

3. Results and discussion

3.1. Structural analysis

Fig. 1 shows the XRD pattern of Ce doped YAG powder subjected to different calcination temperatures. Fig. 1b shows the formation of multiphase product comprising of YAG (JCPDS No. 33-0040), $YAlO_3$ (YAP, JCPD Card No. 33-41) and $Y_4Al_2O_9$ (YAM, JCPD Card No. 34-368) at 800 °C. For sample calcined

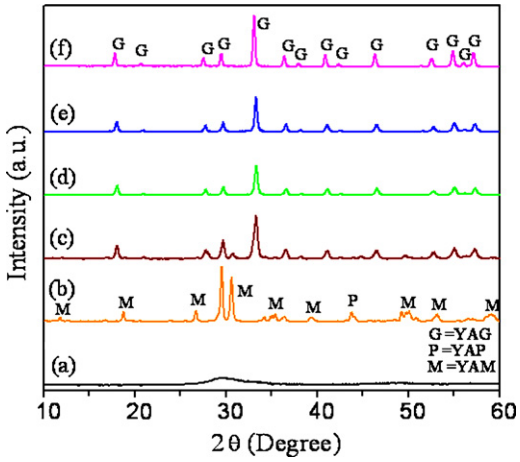

Fig. 1. XRD pattern of Ce doped YAG at different calcination temperatures; (a) 500, (b) 800, (c) 900, (d) 1000, (e) 1100 and (f) 1200 °C.

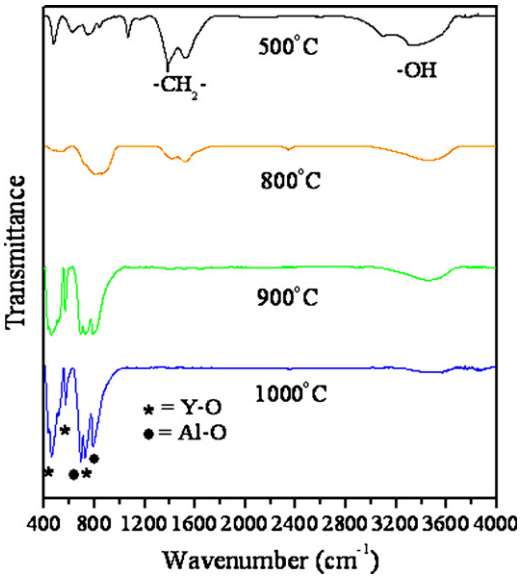

Fig. 2. FTIR spectrum of Ce doped YAG at different calcination temperatures.

at 900 °C, the diffraction pattern indicates the formation of YAG and YAM as shown in Fig. 2c. From Fig. 2d, it is clear that single phase YAG is formed at 1000 °C without any intermediate phases. As shown in the XRD patterns, further calcination at higher temperatures lead to increase in the diffraction peak intensity of Ce doped YAG. It is due to the improvement in degree of crystallization of YAG crystals. It is reported that YAG phase can be obtained at a higher temperature, i.e. above 1600 °C by the conventional solid-state reaction of Y_2O_3–Al_2O_3 binary systems [8]. However, here single phase YAG is produced at a calcination temperature at 1000 °C, which is about 600 °C lower than the conventional solid-state method.

FT-IR spectra of Ce doped YAG powder calcined at various temperatures are shown in Fig. 2. The band near 3500 cm^{-1} is due to the stretching vibration of H_2O. The peaks between 800 and 1500 cm^{-1} might be due to different vibrational and rotational mode of –CH_2–, CO and –COO^- groups. These bands became weaker with increasing calcination temperature and finally disappeared at 800 °C. The peaks at about 790 and 684 cm^{-1} represent the characteristics Al–O (metal–oxygen) vibrations, while the peaks at about 720 and 565 cm^{-1} represent the characteristics Y–O (metal–oxygen) vibrations [19]. The clear separation of Y–O and Al–O peaks at 900 °C suggest that the crystallization of YAG started from 900 °C which is also supported by XRD analyses results.

SEM images of as prepared Ce doped YAG nanoparticles are shown in Fig. 3. The SEM image of precursor powder obtained after solvothermal treatment is shown in Fig. 3a, while the SEM images of calcined sample (at 1000 °C) are

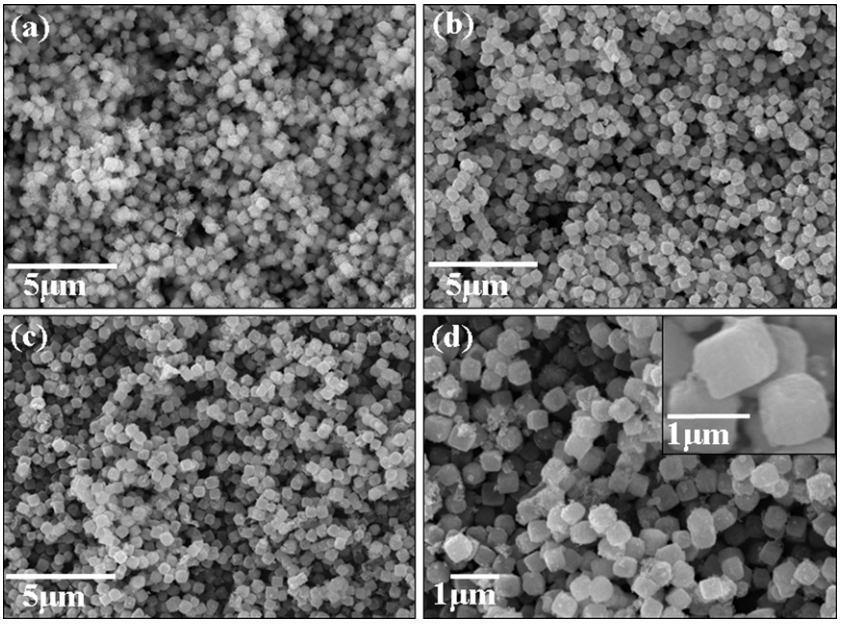

Fig. 3. SEM image of Ce doped YAG nanophosphor; (a) shows the SEM image of precursor powder obtained after solvothermal treatment of the sample while (b), (c) and (d) are the SEM image of Ce doped YAG calcined at 1000 °C.

shown in Fig. 3b–d. SEM images show the formation of monodispersed cubic shape Ce doped YAG nanoparticles. The nanoparticles have regular shape and uniform size distribution. The size of individual cube is 500 nm and the shape and size is nearly unchanged even it is calcined at 1000 °C. As shown in Fig. S-1, the size and shape of commercial Ce doped YAG is not uniform and its size vary from 5 to 20 μm. Compared to commercial sample, Ce doped YAG prepared by present method is in nanometer range and have uniform shape and size distribution. Thus, cubic shape Ce doped YAG may be a suitable candidate for the phosphor application and fabrication of phosphor based white-LED.

The formation mechanism of monodispersed cubic shape Ce doped YAG nanoparticles is investigated by studying the effect of several parameters such as water/ethanol ratio, concentration of surfactant, and different kinds of surfactant. The morphological evolution is only investigated for undoped YAG. First of all, the effect of water/ethanol ratio on the morphology of YAG is investigated, keeping CTAB concentration constant (1 mol %). The corresponding SEM images are shown in Fig. 4 (SEM images are taken for the sample obtained after solvothermal treatment). The SEM images show that mixed solvent is necessary for the formation of monodispersed cubic shape YAG nanoparticles. For example, in Fig. 4a, when pure water is used as solvent, severely agglomerated particles are formed. Although these particles are nearly cubic in shape but their shape and size distribution is not uniform. Furthermore, these particles are larger, about 1 μm, than the Ce doped YAG prepared in mixed solvent. However, when mixed solvent is used, well dispersed cubic shape YAG nanoparticles are formed. For example, when water–ethanol ratio is either 3/4 or 4/3, in both cases, well dispersed, cubic shape particles are formed as shown in Fig. 4b and c, respectively. At the same time, the size of the particles is also decreased, as compared to the size of YAG particles prepared in pure water, and it is comparable to the size of Ce doped YAG nanoparticles. From SEM analyses the average size of YAG nanoparticles was found to be about 500 nm in both cases. However, when pure ethanol is used as solvent, again non-uniform particles are formed having average size of 500 nm (Fig. 4d). Thus, these results suggest that a mixture of water–ethanol is necessary for the formation of monodispersed cubic shape YAG nanoparticles.

The effect of concentration of CTAB on the morphology of YAG particles is investigated by changing the amount of CTAB from 0.5 mol% to 1.5 mol%, keeping the water to ethanol ratio constant (4/3). The SEM images are taken for the sample obtained after solvothermal treatment. Fig. 5a shows that in the absence of CTAB large size and irregular shape YAG particles are formed. It seems that these large particles (∼10 μm) are formed due to the agglomeration of small particles. When 0.5 mol% CTAB is used, large size and agglomerated particles are again formed but these particles are little bit cubic in shape (Fig. 5b). As the concentration of CTAB is increased up to 1 mol% then perfect cubic shape YAG nanoparticles are formed (Fig. 5c). These nanoparticles are well dispersed and uniform in shape as well as size. Further increase in CTAB concentration led to the increase in size as well as agglomeration of particles (Fig. 5d). However, their agglomeration was not due to the aggregation of YAG particles but it was due to high concentration of surfactant which was not removed completely during washing. When this sample was calcined at 500 °C, well dispersed YAG particles are formed (see Fig. S-2). Thus the study suggests that the CTAB played an important role in the formation of cubic structure of YAG particles.

In order to elaborate the role of CTAB in the formation of cubic shape YAG, synthesis was carried out using various kinds of surfactants. For example, when citric acid (1 mol%) is used as the surfactant then spherical shape particles are formed as

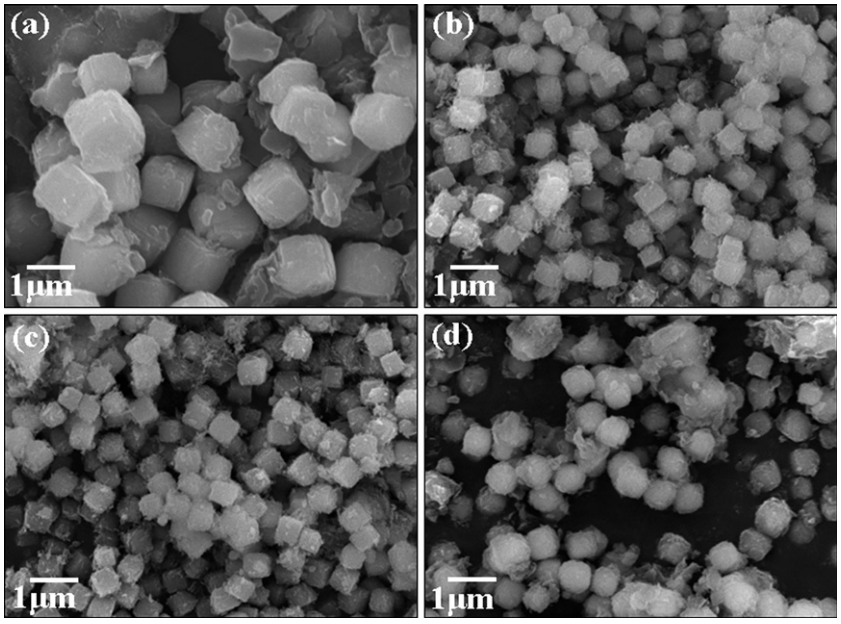

Fig. 4. SEM image of YAG prepared by solvothermal method using different water–ethanol ratio (1 mol% of CTAB); (a) pure water, (b) 20 ml water/15 ml ethanol, (c) 15 ml water/20 ml ethanol and (d) pure ethanol.

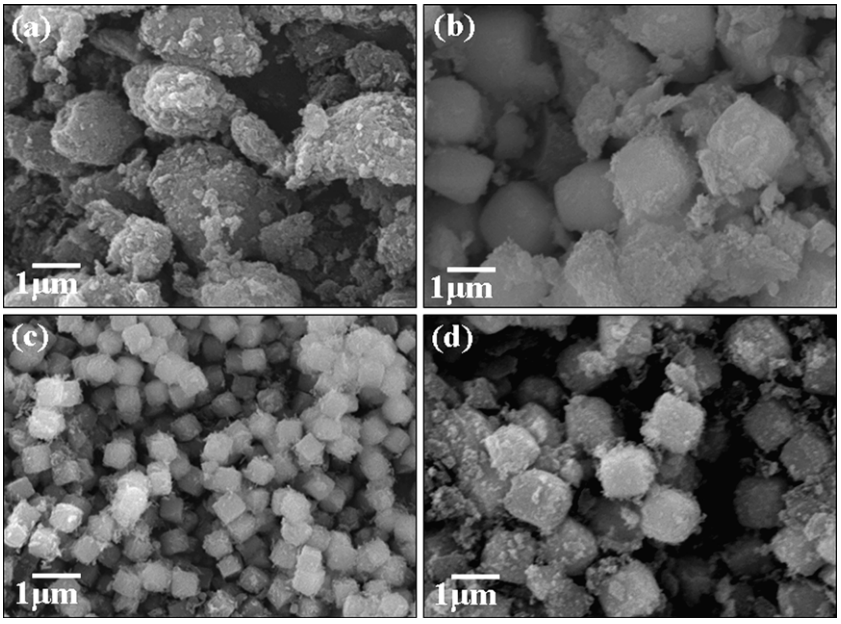

Fig. 5. SEM image of YAG prepared by solvothermal method using different mole% of CTAB; (a) in the absence of CTAB, (b) 0.5 mol % CTAB, (c) 1 mol % CTAB, and (d) 1.5 mol % CTAB.

shown in Fig. 6a. The size distribution of these particles is not uniform and varied from few nanometers to 10 μm. It seems that these microspheres are formed from the aggregation of nanoparticles. However, in the presence of ascorbic acid (1 mol%) different features are observed. As shown in Fig. 6b, only nanoparticles are formed in the presence of ascorbic acid and are uniformly distributed. It means surfactant has a critical role in the modification of shape and size of particles. The importance of two step process over co-precipitation method and solvothermal method is also investigated. The detail experimental procedure is presented in Supplementary Material. When YAG is synthesized by either of the methods alone, non-uniform and agglomerated particles are formed as shown in Fig. 6c and d. The size of these particles varied from 1 μm to 15 μm. However, the particles obtained by co-precipitation method are much bigger than those prepared by solvothermal method as shown in Fig. 6d. It shows that impurity has also a significant effect on the morphology of YAG.

3.2. Growth mechanism

In order to understand the effect of solvent (water and ethanol) and surfactant on phase formation and morphology of YAG, we need to understand the formation mechanism and

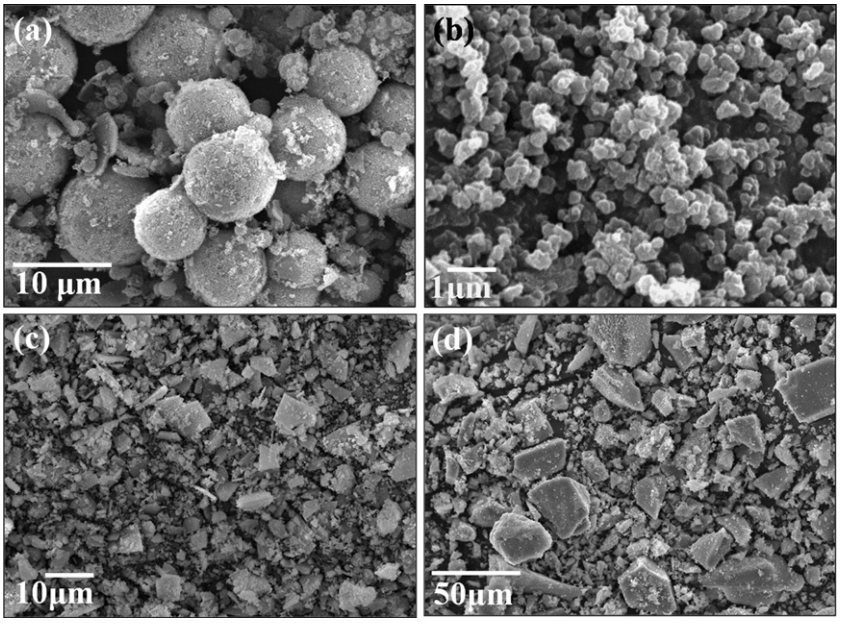

Fig. 6. SEM image of YAG prepared by solvothermal method using different surfactant and methods; (a) citric acid, (b) ascorbic acid, (c) solvothermal method and (d) co-precipitation method.

nature of reaction intermediates. In general, when ammonia water is used as a precipitating agent, Al^{3+} and Y^{3+} ions may be precipitated as $Al(OH)_3$ and $Y(OH)_3$ respectively. Based on above analysis the effect of solvothermal treatment of precursor can be explained as fallows. The precursors used is a mixture of amorphous $Al(OH)_3$ and $Y(OH)_3$, which is weakly polar and has a low solubility in water. Therefore, when an appropriate amount of weakly polar ethyl alcohol is mixed with water, the polarity of the mixed solvent decreased as compared to water and become similar to the polarity of the precursor. This might increase the solubility of the precursor in the mixed solvent. Moreover, the polarity of groups dissolved in the weakly polar solvent would decrease due to the exchange between alkoxy (–OR) and hydroxyl (OH^-) groups, so the migration degree of freedom and collision probability of groups could also increase [20]. As a result, crystals of YAG could be easily formed in the mixed solvent. At the same time the role of surfactant can also be taken in account. CTAB is a cationic surfactant with a hydrophilic head and a long hydrophobic tail. As any surfactant it forms micelles in aqueous solution. CTAB micelles in 0.1 M solution are nearly spherical [21]. Spherical micelles in ionic miceller solution transform to ellipsoidal and cylindrical on addition of additives such as salt, alcohol and amines and this results in increase in viscosity of the solution [22]. The growth rate is different for different additives. Thus, it may be possible that the use of water–ethanol as the solvent could affect the micelle structure of CTAB and hence the growth rate, which resulted in the formation of cube like structure. Furthermore, the long hydrophobic $–CH_2–$ chain absorbed on the surface of the precursor can check the agglomeration between the particles. Therefore, it can be conclude that the solvothermal treatment of precursor precipitate, using CTAB as surfactant, is helpful in the synthesis of cubic shape YAG under mild condition. Considering these factors we can explain the effect of solvent, surfactant and impurity on the morphology of YAG. The change in morphology due to the change in water–ethanol ratio is attributed to the polarity of the solvent. For example, when pure water was used, the polarity of the solvent was high and hence the solubility of weakly polar precursor was low. This caused the aggregation of precursor which resulted into the formation non-uniform particles with agglomeration. However, when ethanol was added, the solubility of precursor increased due to the decrease in polarity of the solvent. This is resulted in the formation of monodispersed cubic shape YAG particles. The formation of non-uniform YAG particles in pure ethanol is not well understood however, it may be due to the low polarity of solvent and hence the low solubility of the precursor.

Similarly the effect of concentration of CTAB on the morphology of cubic shape YAG can be explained as fallows. In the absence of any kind of surfactant ultra fine particles are formed and these particles are agglomerated due to the high pressure of solvent. Thus, it is resulted in the formation of large spheroidal particles. At low concentration of CTAB the complete capping of YAG particle might not be possible and hence agglomeration as well as lack of uniformity in shape and size is observed. As the concentration of CTAB was increased the capping of YAG particle could be more complete and hence well dispersed cubic shape particles are formed.

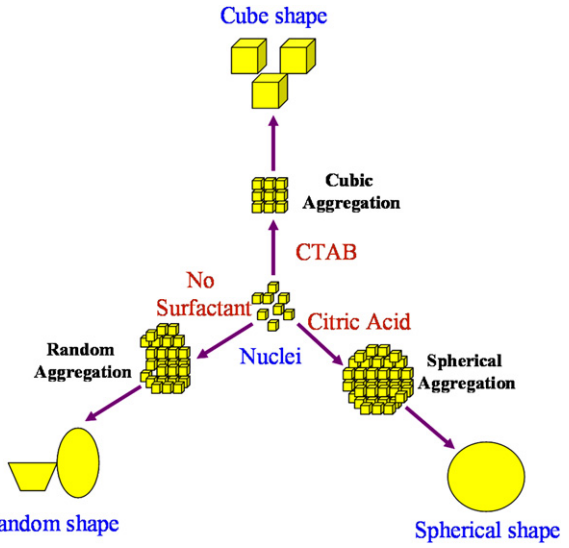

Scheme 1. Growth mechanism of YAG formation in the presence of different surfactants.

However, when CTAB was replaced by citric acid, crystal growth takes place in different manners resulting in spherical shape particles. Since, citric acid has three carboxylic groups and hence it has ability to coordinate at more than one point on the surface of nanoparticles. Furthermore, citric acid is hard to detach from the surface. Therefore, it plays a significant role in the suppression of the particle growth which could decrease the primary particle size. The aggregation of nanoparticles could also occur due to citric acid by the interparticle bridging through the three coordinating sites of the acid molecule. Thus, aggregation of nanoparticles in such a way could lead to the formation of YAG microsphere [23]. Similar interparticle bridging is not possible in the presence of ascorbic acid hence well dispersed YAG nanoparticles are formed. A schematic of growth mechanism of YAG formation in the presence of different surfactants is shown in Scheme 1.

The formation of irregular shape and size particles with agglomeration in case of simple co-precipitation method and solvothermal method suggests that impurity like NH_4^+ and NO_3^- greatly influence the crystal growth. It may be mentioned that counter ions decrease the effective head group area (8 Å) of surfactant molecules (increase in packing parameters, p) by neutralizing the charge on the miceller surface and this could result in the transformation of spherical micelles into other ones [24]. Thus, the above results suggest that the morphology of material is greatly influenced by solvent, surfactant as well as impurity. It also suggests that during the study of effect of any factor like solvent or surfactant on the morphology of materials, the impurity factor should be sorted out to avoid difficulties in understanding the effect of other parameters.

3.3. Photoluminescence property

The photoluminescence spectra of 0.2 mmol of Ce doped YAG powder prepared at various temperatures are shown in

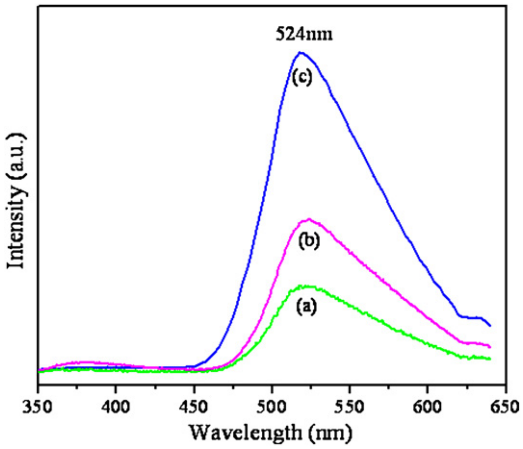

Fig. 7. Photoluminescence spectra of 0.2 mmol of Ce doped YAG powder calcined at different temperatures; (a) 1000, (b) 1100 and (c) 1200 °C.

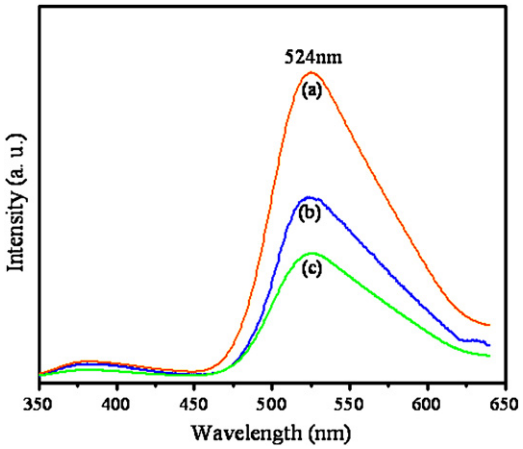

Fig. 8. Emission spectra of Ce doped YAG particles synthesized at 1000 °C for 2 h in air, with different doping concentrations; (a) $x = 0.2$ mmol; (b) $x = 0.4$ mmol; (c) $x = 0.6$ mmol.

Fig. 7. The emission spectra consist of a broad band in the range of 480–640 nm with the maximum intensity at about 524 nm. The emission at 524 nm occurs due to transition from the lowest crystal field component of $5d^1$ to the two levels of the ground state $^2F_{5/2}$ and $^2F_{7/2}$, which are separated by 2000 cm^{-1} due to spin–orbit coupling [25,26]. Emission intensity is one of the most key parameters for the application of Ce-doped YAG phosphor. The analyses show that the calcination temperature profoundly influences the emission intensity. The emission intensity enhanced with increasing annealing temperature without any change in peak position. Emission intensity would generally increase with the annealing temperature due to the increase of crystallinity. As mentioned earlier, the diffraction intensity increased with increasing annealing temperature. The enhancement in emission intensity with increase in annealing temperature could result from the improved crystallization and the decrease of surface defects. Furthermore, annealing may improve the substitution of Ce^{3+} ions into Y lattice in the YAG matrix. The good incorporation of Ce^{3+} ions in the YAG matrix also contributes to the enhancement of emission intensity [27].

Fig. 8 shows the emission spectra of Ce doped YAG particles prepared with different doping concentrations of Ce^{3+} ions. The as prepared particles were calcined at 1000 °C for 2 h. All samples show broad emission peaks in the range 480–640 nm with the maximum intensity at about 524 nm. The emission intensity decreased monotonically with the increase in cerium ion concentration. However, the increase in concentration of cerium ion did not show any kind of shift in peak position. The reduction in emission intensity might be due to the quenching of the electronic transition at higher cerium ion concentration. The luminescent intensity is influenced by the average distance between luminescent centers. As the doping concentration increases, the separation between active ions decreases. At short enough separation the interaction between active ions will occur and cause concentration quenching [11]. Therefore, the homogeneous distribution of active ions in host is essential in order to acquire highly efficient phosphors without concentration quenching.

4. Conclusions

A simple method for the shape selective synthesis of Ce doped YAG nanophosphor has been reported. Monodispersed cubic shape Ce doped YAG nanoparticles have been prepared by solvothermal method using CTAB as a surfactant. Single phase YAG was prepared at much lower calcinations temperature of 1000 °C. The method is helpful in the synthesis of highly dense cubic shape Ce doped YAG in nanometer range and slightly affected by the heat treatment. The growth mechanism suggested that crystal growth depends sensitively on the solvent, surfactant (micelles) and impurity. Additives like solvent and impurity affected the micelle structure which affects the crystal growth and resulted into various kinds of morphologies of YAG. As prepared Ce doped YAG phosphors showed high intensity luminescent peak in the visible region and the intensity increased with the calcination temperature and reduced with increase in cerium ion concentration. The maximum emission wavelength remained unchanged with the calcination temperature and the cerium doping concentration.

Acknowledgements

This study was supported by the Post BK21 program in the Ministry of Education, Human Resources Development, and also supported by the Korea National Research Foundation (NRF) grant funded by the Korea Government (MEST) (NRF-2010-0028802, 2010-0019626).

Appendix A. Supplementary data

Supplementary data associated with this article can be found, in the online version, at doi:10.1016/j.ceramint.2011.06.057.

References

[1] B.H. George, P.R. Linda, Nanophase glass–ceramics, J. Am. Ceram. Soc. 82 (1999) 5–16.

[2] M. Sckita, H. Haneda, S. Shiransaki, T. Yanagitani, Optical spectra of undoped and rare-earth – (=P r, N d, E u, and E r) doped transparent ceramic $Y_3Al_5O_{12}$, J. Appl. Phys. 69 (1991) 3709–3718.
[3] W.H. Chao, R.J. Wu, T.B. Wu, Structural and luminescent properties of YAG:Ce thin film phosphor, J. Alloy Compd. 506 (2010) 98–102.
[4] G. Li, Q. Cao, Z. Li, Y. Huang, Y. Wei, J. Shi, Photoluminescence properties of YAG:Tb nano-powders under vacuum ultraviolet excitation, J. Alloy Compd. 485 (2009) 561–564.
[5] M.L. Saladino, A. Zanotto, D.C. Martino, A. Spinella, G. Nasillo, E. Caponetti, Photoluminescence enhancement of PEG-modified YAG:Ce^{3+} nanocrystal phosphor prepared by glycothermal method, Langmuir 26 (2010) 13442–13449.
[6] C. Huang, J.K. Wu, W.J. Hsu, H.H. Chang, H.Y. Hung, C.L. Lin, H.Y. Su, N. Bagkar, W.C. Ke, H.T. Kuo, R.S. Liu, Particle size effect on the packaging performance of YAG:Ce phosphors in white leds, Int. J. Appl. Ceram. Technol. 6 (2009) 465–469.
[7] X.J. Li, Q.M. Yu, J. Yang, Zh. Zeng, X.P. Jing, Particle growth of $Y_3Al_5O_{12}$:Tb^{3+} phosphor in sol–gel preparation, J. Electrochem. Soc. 154 (2007) H726–H729.
[8] S. Hong, Z. Fu, J. Zhang, S. Zhang, Spectral properties of rare-earth ions in nanocrystalline YAG:Re (Re = Ce^{3+}, Pr^{3+}, Tb^{3+}), J. Lumin. 118 (2006) 179–185.
[9] Y. Sanga, H. Liua, Y. Lva, J. Wanga, T. Chena, D. Liu, X. Zhang, H. Qin, X. Wang, R.I. Boughton, Yttrium aluminum garnet nanoparticles synthesized by nitrate decomposition and their low temperature densification behavior, J. Alloy Compd. 490 (2010) 459–462.
[10] Z. Wu, X. Zhang, W. He, Y. Du, N. Jia, P. Liu, F. Bu, Solvothermal synthesis of spherical YAG powders via different precipitants, J. Alloy Compd. 472 (2009) 576–580.
[11] H. Yang, L. Yuan, G. Zhu, A. Yu, H. Xu, Luminescent properties of YAG:Ce^{3+} phosphor powders prepared by hydrothermal-homogeneous precipitation method, Mater. Lett. 63 (2009) 2271–2273.
[12] Y. Li, J. Zhang, Q. Xiao, R. Zeng, Synthesis of ultrafine spherical YAG:Eu^{3+} phosphors by MOCVD, Mater. Lett. 62 (2008) 3787–3789.
[13] E. Zych, A. Walasek, A.S. Hojniak, Variation of emission color of $Y_3Al_5O_{12}$:Ce induced by thermal treatment at reducing atmosphere, J. Alloy Compd. 451 (2008) 582–585.
[14] A. Purwanto, W.N. Wang, I.W. Lenggoro, K. Okuyama, Formation and luminescence enhancement of agglomerate-free YAG:Ce^{3+} submicrometer particles by flame-assisted spray pyrolysis, J. Electrochem. Soc. 154 (2007) J91–J96.
[15] M.L. Saladino, G. Nasillo, D.C. Martino, E. Caponetti, Synthesis of Nd:YAG nanopowder using the citrate method with microwave irradiation, J. Alloy Compd. 491 (2010) 737–741.
[16] L. Yang, T. Lu, H. Xu, N. Wei, Synthesis of YAG powder by the modified sol–gel combustion method, J. Alloy Compd. 484 (2009) 449–451.
[17] M. Yada, M. Ohya, M. Machida, T. Kijima, Synthesis of porous yttrium aluminium oxide templated by dodecyl sulfate assemblies, Chem. Commun. (1998) 1941–1942.
[18] S. Ye, F. Xiao, Y.X. Pan, Y.Y. Ma, Q.Y. Zhang, Phosphors in phosphor-converted white light-emitting diodes: recent advances in materials, techniques and properties, Mater. Sci. Eng. R 71 (2010) 1–34.
[19] P. Apte, H. Burke, H. Pickup, Synthesis of yttrium aluminum garnet by reverse strike precipitation, J. Mater. Res. 7 (1992) 706–711.
[20] X. Zhang, H. Liu, W. He, J. Wang, X. Li, R.I. Boughton, Synthesis of monodisperse and spherical YAG nanopowder by a mixed solvothermal method, J. Alloy Compd. 372 (2004) 300–303.
[21] P.S. Goyal, S.V.G. Menon, B.A. Dasannacharya, V. Rajagopalan, Role of van der Waals forces on small angle neutron scattering from ionic micellar solutions, Chem. Phys. Lett. 211 (1993) 559–563.
[22] M.E. Cates, S.J. Candau, Statics and dynamics of worm-like surfactant micelles, J. Phys. Condens. Matter 2 (1990) 6869–6892.
[23] R. Asakura, T. Isobe, K. Kurokawa, T. Takagi, H. Aizawa, M. Ohkubo, Effects of citric acid additive on photoluminescence properties of YAG:Ce^{3+} nanoparticles synthesized by glycothermal reaction, J. Lumin. 127 (2007) 416–422.
[24] P.S. Goyal, V.K. Aswal, Micellar structure and inter-micelle interactions in micellar solutions: results of small angle neutron scattering studies, Curr. Sci. 80 (2001) 972–979.
[25] T. Tachiwaki, M. Yoshinaka, Novel synthesis of $Y_3Al_5O_{12}$ (YAG) leading to transparent ceramics, Solid State Commun. 119 (2001) 603–606.
[26] Y. Liu, Z.F. Zhang, B. King, J. Halloran, R.M. Laine, Synthesis of Yttrium aluminum garnet from yttrium and aluminum isobutyrate precursors, J. Am. Ceram. Soc. 79 (1996) 385–394.
[27] A.B. Ageeth, A. Meijerink, Luminescence quantum efficiency of nanocrystalline ZnS:Mn^{2+}. 1. Surface passivation and Mn^{2+} concentration, J. Phys. Chem. B 105 (2001) 10197–10202.